STRUCTURAL BIOLOGY COMMUNICATIONS

ISSN 2053-230X

Purification, crystallization and X-ray crystallographic analysis of a putative exopolyphosphatase from *Zymomonas mobilis*

Aili Zhang,[a] Erhong Guo,[a] Lanfang Qian,[a] Nga-Yeung Tang,[b] Rory M. Watt[b]* and Mark Bartlam[a,c]*

[a]College of Life Sciences, Nankai University, People's Republic of China, [b]Faculty of Dentistry, University of Hong Kong, Hong Kong, and [c]State Key Laboratory of Medicinal Chemical Biology, Nankai University, People's Republic of China. *Correspondence e-mail: rmwatt@hku.hk, bartlam@nankai.edu.cn

Received 4 November 2015
Accepted 14 January 2016

Edited by S. W. Suh, Seoul National University, Korea

Keywords: exopolyphosphatase; PPX/GppA family; crystallization; *Zymomonas mobilis*.

Supporting information: this article has supporting information at journals.iucr.org/f

Exopolyphosphatase (PPX) enzymes degrade inorganic polyphosphate (poly-P), which is essential for the survival of microbial cells in response to external stresses. In this study, a putative exopolyphosphatase from *Zymomonas mobilis* (ZmPPX) was crystallized. Crystals of the wild-type enzyme diffracted to 3.3 Å resolution and could not be optimized further. The truncation of 29 amino acids from the N-terminus resulted in crystals that diffracted to 1.8 Å resolution. The crystals belonged to space group *C*2, with unit-cell parameters $a = 122.0$, $b = 47.1$, $c = 89.5$ Å, $\alpha = \gamma = 90$, $\beta = 124.5^\circ$. An active-site mutant that crystallized in the same space group and with similar unit-cell parameters diffracted to 1.56 Å resolution. One molecule was identified per asymmetric unit. Analytical ultracentrifugation confirmed that ZmPPX forms a dimer in solution. It was confirmed that ZmPPX possesses exopolyphosphatase activity against a synthetic poly-P substrate.

1. Introduction

Inorganic polyphosphate (poly-P), comprising a few to hundreds of orthophosphate residues linked by 'high-energy' phosphoanhydride bonds, is found in virtually all living cells (Kornberg *et al.*, 1999; Hooley *et al.*, 2008; Kumble & Kornberg, 1995). In prokaryotes, these linear polymers play a variety of important physiological functions, including survival and adaption of microbial cells in response to external stresses (such as heat shock, oxidative stress, nutrient depletion and antibiotic treatment; Rao & Kornberg, 1996; Kornberg *et al.*, 1999; Rao *et al.*, 2009). Polyphosphate kinase (PPK) is the principal source of poly-P in most bacteria, whereas exopolyphosphatases (PPX) are mainly responsible for the degradation of poly-P. The alarmones guanosine pentaphosphate (pppGpp) and guanosine tetraphosphate (ppGpp) accumulate during starvation or other stresses (Potrykus & Cashel, 2008). An imbalance between poly-P synthesis and degradation can result in fluctuations of poly-P by 100-fold to 1000-fold; a study in *Escherichia coli* showed that high levels of alarmones have no effect on PPK activity but inhibit PPX activity, resulting in large accumulations of poly-P (Kuroda *et al.*, 1997). PPX enzymes are also essential for virulence, infectivity, resistance, biofilm formation, swimming and swarming motility, and sporulation efficiency (Zhang *et al.*, 2010; Gallarato *et al.*, 2014; Shi *et al.*, 2004; Thayil *et al.*, 2011; Malde *et al.*, 2014).

The PPX/GppA phosphatase family (pfam02541) consists of PPX (EC 3.6.1.11) and guanosine pentaphosphate phosphohydrolase (GppA; EC 3.6.1.40) enzymes (Marchler-Bauer *et al.*, 2015). *E. coli* PPX (EcPPX) and GppA are the best

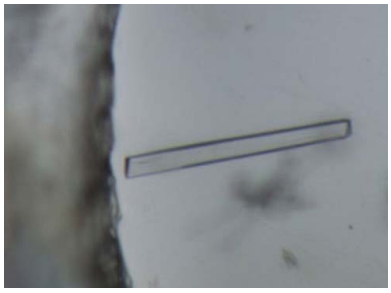

characterized members of the family and both possess dual PPX and GppA activities (Keasling *et al.*, 1993). In contrast, the two PPX/GppA homologues Rv1026 and Rv0496 from *Mycobacterium tuberculosis* possess exopolyphosphatase activity only (Choi *et al.*, 2012; Chuang *et al.*, 2015). PPX/GppA proteins can be divided into 'long' and 'short' homologues. To date, the crystal structures of only two PPX/GppA family proteins have been reported: the 'short' PPX/GppA homologue from *Aquifex aeolicus* (AaPPX) and the 'long' *E. coli* PPX (EcPPX). AaPPX is composed of 312 amino acids and its structure has been determined in complex with the ppGpp alarmone (Kristensen *et al.*, 2004, 2008). Two highly similar dimeric structures of EcPPX have also been reported (Rangarajan *et al.*, 2006; Alvarado *et al.*, 2006). Both AaPPX and EcPPX share conserved catalytic core domains (domains I and II) that are essentially required for exopolyphosphatase activity. Analysis of EcPPX and *Neisseria meningitidis* exopolyphosphatase have identified a highly conserved glutamate (Glu121 in EcPPX) and the Walker B box located in a cleft between domains I and II as essential for exopolyphosphatase activity (Alvarado *et al.*, 2006; Zhang *et al.*, 2010). The 'long' EcPPX features an additional C-terminal poly-P-binding region (domains III and IV) that facilitates processive poly-P hydrolysis and dimer formation (Bolesch & Keasling, 2000). The sequence conservation in this C-terminal region of 'long' PPX/GppA proteins is extremely low.

The *Za10_0559* gene from *Zymomonas mobilis* subsp. *mobilis* NCIMB 11163, a prolific ethanologenic microorganism, encodes a putative exopolyphosphatase (ZmPPX) of 508 amino acids (Kouvelis *et al.*, 2009) that shares 24% sequence identity with EcPPX over 404 aligned residues. *Z. mobilis* is notable for its bioethanol-producing capabilities, which surpass baker's yeast in some respects (Jeffries, 2005; Rogers *et al.*, 2007). Considerable endeavours have been made to obtain antibiotic-sensitive strains and environmental stress-tolerant mutants for industrial applications (Panesar *et al.*, 2006). As intracellular poly-P levels and PPX enzymes are related to stress resistance, determination of the ZmPPX structure should be important for industrial applications of this strain. Furthermore, the determination of its three-dimensional structure should help to elucidate the mechanism of 'long' PPX/GppA enzymes. In this study, we report the expression, purification, crystallization and preliminary analysis of wild-type ZmPPX. The truncation of 29 amino acids from the N-terminus of the protein resulted in a significant improvement in the diffraction of ZmPPX crystals from 3.3 to 1.8 Å resolution using synchrotron radiation. Crystals of an active-site mutant protein bearing an alanine substitution for the conserved residue Glu137 (corresponding to Glu121 in EcPPX) were also grown and diffracted to 1.56 Å resolution.

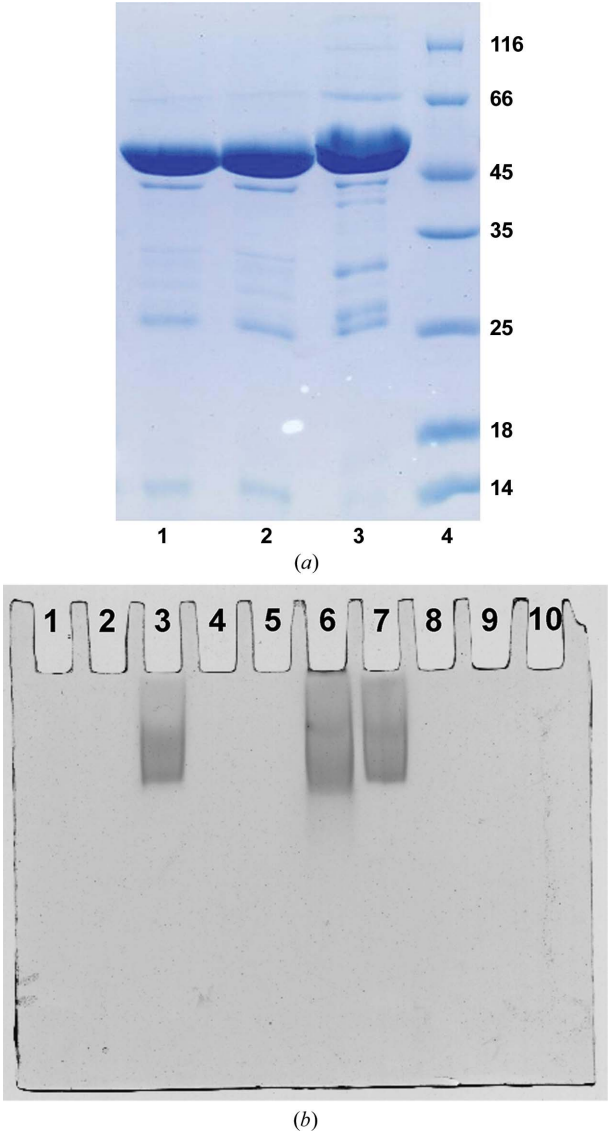

Figure 1
(*a*) 13% SDS–PAGE analysis of the purified ZmPPX(30–508) protein (lane 1), ZmPPX(30–508) E137A mutant (lane 2) and full-length ZmPPX protein (lane 3) used for crystallization trials. Molecular-weight markers are labelled in kDa (lane 4). (*b*) Exopolyphosphatase activity assay of ZmPPX against a long-chain polyphosphate substrate (poly-P_{130}). Lane 3, protein-free negative control; lane 4, full-length ZmPPX; lane 5, ZmPPX(30–508); lane 6, ZmPPX(30–508) E137A mutant; lane 7, poly-P_{130} substrate without inhibition. Lanes 1, 2, 8, 9 and 10 were left empty.

2. Materials and methods

2.1. Macromolecule production

The full-length ZmPPX protein was amplified from the full-length *Za10_0559* gene PCR-amplified from genomic DNA purified from *Z. mobilis* subsp. *mobilis* NCIMB 11163. The forward and reverse primers were 5′-CGGGATCCATGATATTGAATAACAGGCAGG-3′ (the BamHI site is underlined) and 5′-CCGCTCGAGTTATAAAAATTCGACCACTTCG-3′ (the XhoI site is underlined), respectively. From multiple sequence alignment of ZmPPX with other homologues belonging to the PPX/GppA family (Supplementary Fig. S1) and prediction using the Conserved Domain Database in NCBI (Marchler-Bauer *et al.*, 2015), the DNA sequence encoding ZmPPX from residues 30 to 508 [hereafter termed ZmPPX(30–508)] was amplified from the full-length *Za10_0559* gene by PCR. The forward primer and the reverse

Table 1
Macromolecule-production information.

Protein	ZmPPX	ZmPPX(30–508)	ZmPPX(30–508) E137A mutant
Source organism	*Z. mobilis* subsp. *mobilis* NCIMB 11163 (GenBank accession No. CP001722.1)	*Z. mobilis* subsp. *mobilis* NCIMB 11163 (GenBank accession No. CP001722.1)	*Z. mobilis* subsp. *mobilis* NCIMB 11163 (GenBank accession No. CP001722.1)
DNA source	Plasmid	Plasmid	Plasmid
Forward primer	CGGGATCCATGATATTGAATAACAGGCAGG†	CGGGATCCATCGGTATCATTGATATTGGTT†	TCTTGTCGGGCGAAGAAGCGGGCTATGCT‡
Reverse primer	CCGCTCGAGTTATAAAAATTCGACCACTTCG§	CCGCTCGAGTTATAAAAATTCGACCACTTCG§	GCTTCTTCGCCCGACAAGACTTCAACTTC‡
Cloning vector	Modified pET-32a¶	Modified pET-32a	Modified pET-32a
Expression vector	Modified pET-32a	Modified pET-32a	Modified pET-32a
Expression host	*E. coli* BL21 (DE3)	*E. coli* BL21 (DE3)	*E. coli* BL21 (DE3)
Complete amino-acid sequence of the construct produced††	GPGSMILNNRQGSNDVDKKCPMPKQKKWCKSGPI-GIIDIDGSNSIRLVVYDQLSRAPRILFNEKISA-QLGRNIPVDGRIDEKAIELAISELTRFWKLAQ-IMELSSLRTVATAAVRDAKNGAFLLGEIAKIG-LEVEVLSGEEEGYASGYGVLSAIPDADGIVGD-LGGGSLELIRVSKGRVKDRVSLPLGVLRIADI-RKKSRNALDNFISEAFKKIDWLADARDLPFYM-VGGAWRSLAKLDMHVRHYPIPVLHNYIMSPDR-PSKLIRVIQRNNPKKLKNKANISTSRVEQLSD-AAALLAVVSRHLHSRALVTSAYGLREGLLYLS-LDKATRKLDPLLWSANQRGETAGRFYQQGEAL-YDWMSTLFAQDPPAYHRLRHAACLLADSAWQA-NPDFRAEQILSIILHGRWVGLDAYGRALIGQA-LAVSYDGAMDKKITNNLLSEADTIRAVRWGKA-IRLGMRLSGGVTTSLKKSTILYRNNKIILQFS-GNYKLKGETVLRRLRSLASSFEASEVVEFL	GPGSIGIIDIDGSNSIRLVVYDQLSRAPRILFNEK-ISAQLGRNIPVDGRIDEKAIELAISELTRFWK-LAQIMELSSLRTVATAAVRDAKNGAFLLGEIA-KIGLEVEVLSGEEEGYASGYGVLSAIPDADGI-VGDLGGGSLELIRVSKGRVKDRVSLPLGVLRI-ADIRKKSRNALDNFISEAFKKIDWLADARDLP-FYMVGGAWRSLAKLDMHVRHYPIPVLHNYIMS-PDRPSKLIRVIQRNNPKKLKNKANISTSRVEQ-LSDAAALLAVVSRHLHSRALVTSAYGLREGLL-YLSLDKATRKLDPLLWSANQRGETAGRFYQQG-EALYDWMSTLFAQDPPAYHRLRHAACLLADSA-WQANPDFRAEQILSIILHGRWVGLDAYGRALI-GQALAVSYDGAMDKKITNNLLSEADTIRAVRW-GKAIRLGMRLSGGVTTSLKKSTILYRNNKIIL-QFSGNYKLKGETVLRRLRSLASSFEASEVVEFL	GPGSIGIIDIDGSNSIRLVVYDQLSRAPRILFNEK-ISAQLGRNIPVDGRIDEKAIELAISELTRFWK-LAQIMELSSLRTVATAAVRDAKNGAFLLGEIA-KIGLEVEVLSGEEEGYASGYGVLSAIPDADGI-VGDLGGGSLELIRVSKGRVKDRVSLPLGVLRI-ADIRKKSRNALDNFISEAFKKIDWLADARDLP-FYMVGGAWRSLAKLDMHVRHYPIPVLHNYIMS-PDRPSKLIRVIQRNNPKKLKNKANISTSRVEQ-LSDAAALLAVVSRHLHSRALVTSAYGLREGLL-YLSLDKATRKLDPLLWSANQRGETAGRFYQQG-EALYDWMSTLFAQDPPAYHRLRHAACLLADSA-WQANPDFRAEQILSIILHGRWVGLDAYGRALI-GQALAVSYDGAMDKKITNNLLSEADTIRAVRW-GKAIRLGMRLSGGVTTSLKKSTILYRNNKIIL-QFSGNYKLKGETVLRRLRSLASSFEASEVVEFL

† The BamHI site is underlined. ‡ The mutant site is underlined. § The XhoI site is underlined. ¶ Contains only the N-terminal 6×His tag and a PreScission Protease cleavage site. †† Non-native residues originating from the expression vector are underlined.

primer were 5′-CGGGATCCATCGGTATCATTGATATTG-GTT-3′ (the BamHI site is underlined) and 5′-CCGCTCGAG-TTATAAAAATTCGACCACTTCG-3′ (the XhoI site is underlined), respectively. The resulting PCR product was digested with BamHI and XhoI, and then ligated into an in-house-modified version of the pET-32a vector (Novagen), which expresses the protein with an N-terminal 6×His tag followed by a PreScission Protease cleavage site (LEVL-FQGP). The plasmid for the ZmPPX(30–508) E137A mutant was obtained by PCR using the Fast Mutagenesis system (TransGen, China) according to the manufacturer's instructions. The amplified sequences of all genes were verified by DNA sequencing (AuGCT, China).

The recombinant plasmids were transformed into *E. coli* strain BL21(DE3) and the cells were cultured in LB medium containing 100 mg l^{-1} ampicillin to an OD_{600} of 0.6 at 310 K. Protein expression was induced with 0.5 m*M* IPTG (isopropyl *β*-D-1-thiogalactopyranoside) at 289 K for 18 h. The cells were harvested by centrifugation at 5000*g* for 15 min, resuspended in buffer *P* [50 m*M* Tris pH 8.0, 500 m*M* NaCl, 5%(*v*/*v*) glycerol] and lysed by sonication at 277 K. The crude extracts were then centrifuged at 18 000*g* for 45 min at 277 K to remove the cell debris. The supernatant containing the protein was loaded onto an Ni^{2+}-chelating affinity column (2.0 ml Ni^{2+}–NTA agarose, GE Healthcare, USA) pre-equilibrated with buffer *P* and then washed with buffer *P* containing 30 m*M* imidazole (five column volumes). The bound 6×His-tagged fusion protein was eluted with buffer *P* containing 300 m*M* imidazole. The eluate was concentrated by ultrafiltration and buffer-exchanged into buffer *P*. After digestion overnight at 277 K with PreScission Protease, the protein mixture was subjected to a Superdex 200 size-exclusion chromatography column (GE Healthcare, USA) equilibrated in buffer *P* for further purification and removal of the 6×His tag. The purities of all proteins were greater than approximately 98% as determined by SDS–PAGE analysis (Fig. 1*a*). The full-length ZmPPX protein was concentrated to 10 mg ml^{-1} and truncated ZmPPX proteins were concentrated to 8 mg ml^{-1} for subsequent crystallization trials. Information on macromolecule production is summarized in Table 1.

Analytical sedimentation-velocity experiments using ZmPPX(30–508) were carried out at 277 K with a Beckman XL-I analytical ultracentrifuge equipped with an An-60 Ti rotor. Data were obtained at 36 000 rev min^{-1} using 390 µl protein at 1 mg ml^{-1}. The data were acquired using an interferometer system. The *SEDFIT* program was used for data analysis to estimate the molar mass and sedimentation coefficient.

Exopolyphosphatase assays were performed as described by Choi *et al.* (2012). Briefly, the reactions (50 µl) consisted of 50 m*M* HEPES pH 6.8, 25 m*M* KCl, 10 m*M* $MgCl_2$, polyphosphate substrate (poly-P_{130}; generously supplied by Dr T. Shiba, RegeneTiss Ltd, Japan) and 2 µ*M* of the indicated protein, and were incubated at 310 K for 2 h. Loading dye (25 µl) was added (1 × TBE, 10% sucrose, 0.05% bromophenol blue) and 25 µl aliquots were analyzed on 12% TBE–polyacrylamide gels, staining the polyphosphate products using toluidine blue (Fig. 1*b*).

2.2. Crystallization

A preliminary crystallization screen was conducted for the full-length ZmPPX protein using the hanging-drop vapour-diffusion method with Crystal Screen, Crystal Screen 2 and

Table 2
Crystallization.

Protein	ZmPPX	ZmPPX(30–508)	ZmPPX(30–508) E137A mutant
Method	Hanging-drop vapour diffusion	Sitting-drop vapour diffusion	Sitting-drop vapour diffusion
Plate type	48-well plates	48-well plates	48-well plates
Temperature (K)	293	293	293
Protein concentration (mg ml^{-1})	10	8	8
Buffer composition of protein solution	50 m*M* Tris pH 8.0, 500 m*M* NaCl, 5% glycerol	50 m*M* Tris pH 8.0, 500 m*M* NaCl, 5% glycerol	50 m*M* Tris pH 8.0, 500 m*M* NaCl, 5% glycerol
Composition of reservoir solution	15.2%(*w*/*v*) polyethylene glycol 3350, 2%(*w*/*v*) polyethylene glycol 8000, 72 m*M* Tris pH 8.0, 144 m*M* magnesium chloride hexahydrate, 20 m*M* HEPES/sodium hydroxide pH 7.5, 1.6%(*v*/*v*) glycerol, 8%(*v*/*v*) DMSO	0.2 *M* magnesium chloride hexahydrate, 0.1 *M* Tris pH 8.5, 25%(*w*/*v*) polyethylene glycol 3350	0.2 *M* magnesium chloride hexahydrate, 0.1 *M* Tris pH 6.5, 25%(*w*/*v*) polyethylene glycol 3350
Volume and ratio of drop	3 µl in total, 2:1	2 µl in total, 1:1	2 µl in total, 1:1
Volume of reservoir (µl)	200	100	100

Table 3
Data collection and processing.

Values in parentheses are for the outer shell.

Protein	ZmPPX	ZmPPX(30–508)	ZmPPX(30–508) E137A mutant
Diffraction source	BL-17U1, SSRF	BL-19U1, SSRF	BL-17A, KEK
Wavelength (Å)	0.98	0.98	0.98
Temperature (K)	100	100	100
Detector	ADSC Quantum 315r	Pilatus 6M	ADSC Quantum 270
Crystal-to-detector distance (mm)	400.0	300.0	295.0
Rotation range per image (°)	0.5	0.5	0.5
Total rotation range (°)	180	267	180
Space group	*P*2	*C*2	*C*2
a, *b*, *c* (Å)	58.3, 104.1, 242.2	122.0, 47.1, 89.5	122.7, 47.9, 94.9
α, β, γ (°)	90.0, 92.3, 90.0	90.0, 124.5, 90.0	90.0, 126.5, 90.0
Resolution range (Å)	50.0–3.30 (3.42–3.30)	50.0–1.80 (1.84–1.80)	50.0–1.56 (1.59–1.56)
Total No. of reflections	162804	156187	206483
No. of unique reflections	43109 (4335)	38980 (2498)	63367 (3094)
Completeness (%)	98.5 (99.1)	98.9 (96.3)	99.6 (98.2)
Multiplicity	3.8 (3.8)	4.0 (3.1)	3.3 (2.9)
$\langle I/\sigma(I)\rangle$	16.8 (2.5)	11.6 (2.0)	26.2 (3.1)
$R_{\rm meas}$	0.086 (0.499)	0.136 (0.620)	0.051 (0.375)
Overall *B* factor from Wilson plot (Å^2)	44.4	20.3	10.5

Index kits (Hampton Research, USA) at 293 K. Small crystals were obtained from Index condition No. 85 [0.2 *M* magnesium chloride hexahydrate, 0.1 *M* Tris pH 8.5, 25%(*w*/*v*) polyethylene glycol 3350]. Initial crystallization conditions were optimized manually and the single crystals that were used for diffraction were grown under optimized conditions consisting of 15.2%(*w*/*v*) PEG 3350, 2%(*w*/*v*) PEG 8000, 72 m*M* Tris pH 8.0, 144 m*M* magnesium chloride hexahydrate, 20 m*M* HEPES/sodium hydroxide pH 7.5, 1.6%(*v*/*v*) glycerol, 8%(*v*/*v*) DMSO. The protein concentration was 10 mg ml^{-1} and the volumes of protein and reservoir solution were 2 and 1 µl, respectively.

Crystallization experiments on the N-terminally truncated ZmPPX(30–508) protein and the ZmPPX(30–508) E137A mutant protein were performed by the sitting-drop vapour-diffusion method using Crystal Screen, Crystal Screen 2 and Index (Hampton Research, USA) to screen for crystals at 293 K. Both proteins were crystallized by mixing 1 µl protein solution with 1 µl reservoir solution and equilibrating against 100 µl reservoir solution in 48-well plates (Tianjin Xiangyushun Macromolecule Technology Ltd, People's Republic of China). Diffraction-quality crystals of ZmPPX(30–508) and E137A mutant proteins were typically obtained ∼5 d later from Index conditions No. 85 [0.2 *M* magnesium chloride hexahydrate, 0.1 *M* Tris pH 8.5, 25%(*w*/*v*) polyethylene glycol 3350] and No. 83 [0.2 *M* magnesium chloride hexahydrate, 0.1 *M* Tris pH 6.5, 25%(*w*/*v*) polyethylene glycol 3350]. respectively. Crystallization information is summarized in Table 2.

2.3. Data collection and processing

Crystals were transferred to cryoprotectant [reservoir solution mixed with 25%(*v*/*v*) glycerol] and immediately flash-cooled in liquid nitrogen at 100 K prior to data collection. X-ray diffraction data for full-length ZmPPX were collected on beamline BL-17U1 (100 K, λ = 0.978 Å) at Shanghai Synchrotron Radiation Facility (SSRF). Data for ZmPPX(30–508) were collected on beamline BL-19U1 (100 K, λ = 0.978 Å) at SSRF. Data for the E137A active-site mutant of ZmPPX(30–508) were collected on beamline BL-17A (100 K, λ = 0.980 Å) at the Photon Factory (KEK, Japan). All data were indexed, integrated and scaled using the *HKL*-2000 package (Otwinowski & Minor, 1997). The initial phases were

obtained *via* the molecular-replacement program *BALBES* (Long *et al.*, 2008). Data-collection statistics are summarized in Table 3.

3. Results and discussion

Our attempts to crystallize the full-length ZmPPX protein resulted in crystals that diffracted to a maximum resolution of 3.3 Å using synchrotron radiation (Fig. 2). The protein was crystallized in space group *P*2 and the data were processed with unit-cell parameters a = 58.3, b = 104.1, c = 242.2 Å, $\alpha = \gamma = 90$, $\beta = 92.3^{\circ}$. Matthews coefficient analysis of the full-length ZmPPX crystals predicted the presence of five or six molecules in the asymmetric unit, with V_M values and solvent contents of 2.60 Å^3 Da^{-1} and 53% and of 2.17 Å^3 Da^{-1} and 43%, respectively. Further optimization of the crystallization conditions could not improve the resolution of diffraction, and therefore it was decided to investigate other methods. We used primary-sequence analysis to truncate the N-terminal 29 amino acids based on an alignment with other PPX/GppA family homologues *via* their conserved N-terminal domains (Supplementary Fig. S1). The truncated ZmPPX(30–508) protein was successfully expressed using an in-house-modified version of the pET-32a vector (Novagen) with an N-terminal 6×His tag followed by a PreScission Protease cleavage site (LEVLFQGP). An E137A active-site mutant of ZmPPX(30–508) was also expressed for subsequent ligand-binding experiments and for crystallographic analysis of substrate-bound or product-bound proteins.

The exopolyphosphatase activities of the ZmPPX(1–508), ZmPPX(30–508) and ZmPPX(30–508) E137A proteins were determined by incubating them with a synthetic polyphosphate (poly-P) substrate with an average chain length of 130 units (poly-P_{130}) and analyzing the products on a 12% TBE–polyacrylamide gel (Choi *et al.*, 2012). As can be clearly seen in the gel image shown in Fig. 1(*b*), both the full-length ZmPPX protein (lane 4) and the ZmPPX(30–508) protein (lane 5) have efficient exopolyphosphatase activity against the long-chain polyphosphate substrate (poly-P_{130}), suggesting that truncation of the N-terminal residues does not affect the activity. Under the conditions employed, no detectable polyphosphate remained after 90 min incubation at 310 K. In contrast, the ZmPPX(30–508) E137A mutant protein (lane 6) appears to completely lack exopolyphosphatase activity. The protein-free negative control is shown in lane 3 and the poly-P_{130} substrate (without incubation) is shown in lane 7. Lanes 1, 2, 8, 9 and 10 were left empty.

Both the ZmPPX(30–508) and ZmPPX(30–508) E137A mutant proteins were crystallized from a similar condition consisting of 0.2 *M* magnesium chloride hexahydrate, 0.1 *M*

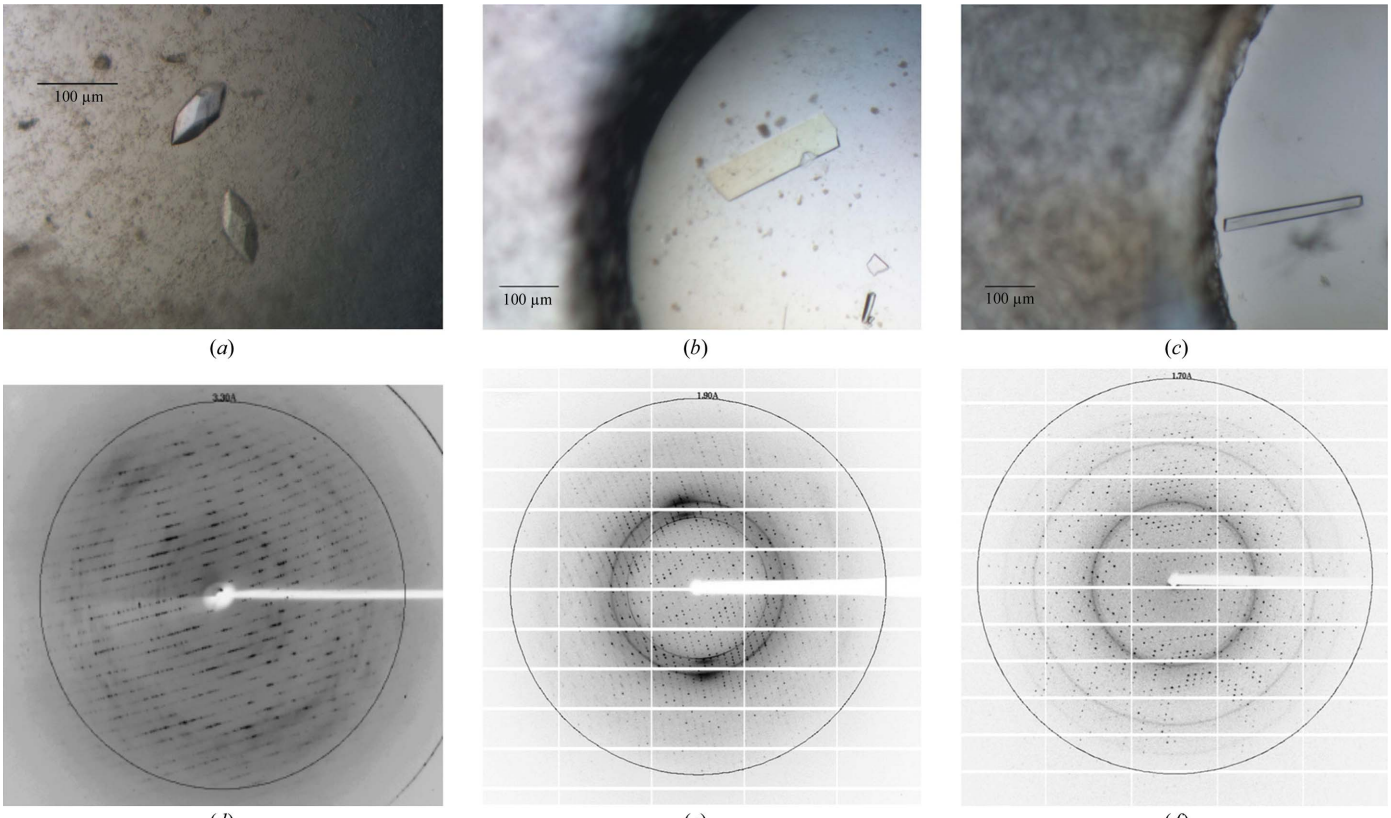

Figure 2
(*a*) Crystals of ZmPPX. The scale bar represents 100 µm. (*b*) Crystal of ZmPPX(30–508). The scale bar represents 100 µm. (*c*) Crystal of ZmPPX(30–508) E137A mutant. The scale bar represents 100 µm. (*d*) Representative diffraction pattern for ZmPPX. The outer ring represents 3.3 Å resolution. (*e*) Representative diffraction pattern for ZmPPX(30–508). The outer ring represents 1.9 Å resolution. (*f*) Representative diffraction pattern for ZmPPX(30–508) E137A mutant. The outer ring represents 1.7 Å resolution.

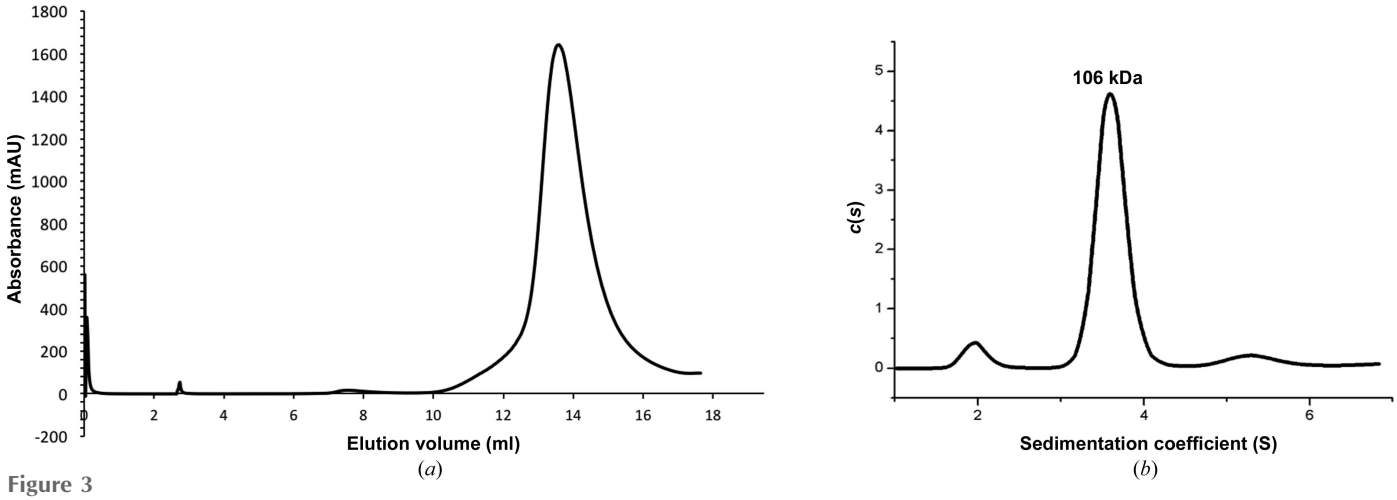

Figure 3
The Superdex 200 size-exclusion chromatography profile (*a*) and analytical ultracentrifugation (AUC) analysis (*b*) suggest that ZmPPX(30–508) exists as a dimer in solution. The significant AUC peak corresponds to the molecular weight of a dimer (106 kDa = 53 kDa × 2).

Tris, 25%(*w*/*v*) polyethylene glycol 3350, albeit at different pH values: pH 8.5 for the wild-type protein and pH 6.5 for the E137A mutant (Fig. 2). Both proteins were crystallized in space group *C*2 and the data were processed with unit-cell parameters $a = 122.0$, $b = 47.1$, $c = 89.5$ Å, $\alpha = \gamma = 90$, $\beta = 124.5^\circ$ for the native protein and $a = 122.7$, $b = 47.9$, $c = 94.9$ Å, $\alpha = \gamma = 90$, $\beta = 126.5^\circ$ for the mutant. Diffraction data were collected to high resolution using the $\langle I/\sigma(I)\rangle$ value as a guide without significantly sacrificing the completeness in the outer resolution shells (Table 3).

Matthews coefficient analysis of ZmPPX crystals suggested the presence of one molecule in an asymmetric unit, with a V_M value of 1.99 Å^3 Da^{-1} and an estimated solvent content of 38%. As the C-terminal domains of 'long' PPX proteins are predicted to be involved in dimer formation, we characterized the protein by size-exclusion chromatography (Fig. 3*a*) and analytical ultracentrifugation (AUC; Fig. 3*b*). Both results indicate that ZmPPX exists as a dimer in solution, with the significant AUC peak corresponding to 106 kDa, which is consistent with the molecular weight of a dimer (Fig. 3*b*). Initial phases were calculated by molecular replacement using *BALBES* (Long *et al.*, 2008). The only solution was obtained using the structure of the putative exopolyphosphatase from *Agrobacterium tumefaciens* strain C58 (PDB entry 3hi0; Joint Center for Structural Genomics, unpublished work), which shares 37% sequence identity with ZmPPX over 415 aligned residues, as a search model. Refinement of the molecular-replacement solution using *REFMAC* (Murshudov *et al.*, 2011) gave an initial R_{work} and R_{free} of 39.0 and 45.4%, respectively, suggesting the correctness of the solution. Full structural and functional analysis of ZmPPX is currently under way and will be reported elsewhere.

4. Related literature

The following references are cited in the Supporting Information for this article: Goujon *et al.* (2010) and Robert & Gouet (2014).

Acknowledgements

This work was supported by the National Science Foundation of China (grant No. 31570128 to MB) and the Research Grants Council of Hong Kong through the General Research Fund (GRF; grant No. 17121814). We thank Zuokun Lu for technical assistance.

References

Alvarado, J., Ghosh, A., Janovitz, T., Jauregui, A., Hasson, M. S. & Sanders, D. A. (2006). *Structure*, **14**, 1263–1272.
Bolesch, D. G. & Keasling, J. D. (2000). *J. Biol. Chem.* **275**, 33814–33819.
Choi, M. Y., Wang, Y., Wong, L. L. Y., Lu, B.-T., Chen, W.-Y., Huang, J.-D., Tanner, J. A. & Watt, R. M. (2012). *PLoS One*, **7**, e42561.
Chuang, Y.-M., Bandyopadhyay, N., Rifat, D., Rubin, H., Bader, J. S. & Karakousis, P. C. (2015). *MBio*, **6**, e02428.
Gallarato, L. A., Sánchez, D. G., Olvera, L., Primo, E. D., Garrido, M. N., Beassoni, P. R., Morett, E. & Lisa, A. T. (2014). *Microbiology*, **160**, 406–417.
Goujon, M., McWilliam, H., Li, W., Valentin, F., Squizzato, S., Paern, J. & Lopez, R. (2010). *Nucleic Acids Res.* **38**, W695–W699.
Hooley, P., Whitehead, M. P. & Brown, M. R. (2008). *Trends Biochem. Sci.* **33**, 577–582.
Jeffries, T. W. (2005). *Nature Biotechnol.* **23**, 40–41.
Keasling, J. D., Bertsch, L. & Kornberg, A. (1993). *Proc. Natl Acad. Sci. USA*, **90**, 7029–7033.
Kornberg, A., Rao, N. N. & Ault-Riché, D. (1999). *Annu. Rev. Biochem.* **68**, 89–125.
Kouvelis, V. N., Saunders, E., Brettin, T. S., Bruce, D., Detter, C., Han, C., Typas, M. A. & Pappas, K. M. (2009). *J. Bacteriol.* **191**, 7140–7141.
Kristensen, O., Laurberg, M., Liljas, A., Kastrup, J. S. & Gajhede, M. (2004). *Biochemistry*, **43**, 8894–8900.
Kristensen, O., Ross, B. & Gajhede, M. (2008). *J. Mol. Biol.* **375**, 1469–1476.
Kumble, K. D. & Kornberg, A. (1995). *J. Biol. Chem.* **270**, 5818–5822.
Kuroda, A., Murphy, H., Cashel, M. & Kornberg, A. (1997). *J. Biol. Chem.* **272**, 21240–21243.
Long, F., Vagin, A. A., Young, P. & Murshudov, G. N. (2008). *Acta Cryst.* D**64**, 125–132.
Malde, A., Gangaiah, D., Chandrashekhar, K., Pina-Mimbela, R., Torrelles, J. B. & Rajashekara, G. (2014). *Virulence*, **5**, 521–533.
Marchler-Bauer, A. *et al.* (2015). *Nucleic Acids Res.* **43**, D222–D226.

Murshudov, G. N., Skubák, P., Lebedev, A. A., Pannu, N. S., Steiner, R. A., Nicholls, R. A., Winn, M. D., Long, F. & Vagin, A. A. (2011). *Acta Cryst.* D**67**, 355–367.
Otwinowski, Z. & Minor, W. (1997). *Methods Enzymol.* **276**, 307–326.
Panesar, P. S., Marwaha, S. S. & Kennedy, J. F. (2006). *J. Chem. Technol. Biotechnol.* **81**, 623–635.
Potrykus, K. & Cashel, M. (2008). *Annu. Rev. Microbiol.* **62**, 35–51.
Rangarajan, E. S., Nadeau, G., Li, Y., Wagner, J., Hung, M.-N., Schrag, J. D., Cygler, M. & Matte, A. (2006). *J. Mol. Biol.* **359**, 1249–1260.
Rao, N. N., Gómez-García, M. R. & Kornberg, A. (2009). *Annu. Rev. Biochem.* **78**, 605–647.
Rao, N. N. & Kornberg, A. (1996). *J. Bacteriol.* **178**, 1394–1400.
Robert, X. & Gouet, P. (2014). *Nucleic Acids Res.* **42**, W320–W324.
Rogers, P. L., Jeon, Y. J., Lee, K. J. & Lawford, H. G. (2007). *Adv. Biochem. Eng. Biotechnol.* **108**, 263–288.
Shi, X., Rao, N. N. & Kornberg, A. (2004). *Proc. Natl Acad. Sci. USA*, **101**, 17061–17065.
Thayil, S. M., Morrison, N., Schechter, N., Rubin, H. & Karakousis, P. C. (2011). *PLoS One*, **6**, e28076.
Zhang, Q., Li, Y. & Tang, C. M. (2010). *J. Biol. Chem.* **285**, 34259–34268.